From the Southern Ocean to the North Atlantic in the Ekman layer?

Doron Nof *

and

Agatha de Boer

Department of Oceanography 4320
The Florida State University
Tallahassee, Florida 32306-4320 U.S.A.
nof@ocean.fsu.edu

* *Also affiliated with The Geophysical Fluid Dynamics Institute, Florida State University*

September, 2002

Contrary to common perceptions, most of the meridional transfer of water from the Southern Ocean to the northern hemisphere does not correspond to the Ekman flux in the Southern Ocean.

Abstract

Since the Southern Ocean encompasses the entire circumference of the globe, the zonal integral of the pressure gradient vanishes implying that the (meridional) geostrophic mass flux is zero. Conventional wisdom has it that, in view of this, the northward Ekman flux there must somehow find its way to the northern oceans, sink to the bottom (due to cooling) and return southward below the topography. Using recent (process oriented) numerical simulations and a simple analytical model, it is shown that most of the Ekman flux in the Southern Ocean does not cross the equator, nor does it sink in the northern oceans. Rather, the water that constitutes the link between the Southern Ocean and the deep water formation in the northern hemisphere originates in the eastern part of the southern Sverdrup interior.

The associated path which takes the water from one hemisphere to the other resembles the letter "S," where the top of the letter corresponds to the sinking region in the northern hemisphere and the bottom to the origin in the Southern Ocean. Although it is true that the *amount* of water that is crossing the equator is equal to the integrated Ekman flux in the northernmost part of the Southern Ocean, it is merely the amount (and not the origin of the water) that is equal in the two cases. The width of the trans-hemispheric current in the south is $\beta\tau L/\rho_0(\partial\tau/\partial y)$, where τ is the wind stress, $\partial\tau/\partial y$ the curl of the wind, β the familiar variation of the Coriolis with latitude, ρ_0 the mean seawater density, and L is the width of the basin.

Introduction

The idea that the southern winds might be important to the rate of the deep water formation in the North Atlantic was first put forward by Toggweiler and Samuels (1995). They analyzed the results of a global circulation model (GCM) and showed that the rate of North Atlantic Deep Water formation (NADW) increased when the strength of the southern winds was increased. Since a zonal integration of the geostrophic pressure associated with the interior (i.e., the domain below the top Ekman layer and above bottom topography) over the Southern Ocean vanishes, and since there can be no local transformation of Ekman water to deep water, they concluded that the transformation must take place in the North Atlantic via the NADW. In this scenario, the Ekman flux in the Southern Ocean must somehow find its way to the northern hemisphere where, through cooling, it sinks to the bottom. We shall show here that, although the mass flux of water crossing the equator is indeed equal to the Ekman flux in the Southern Ocean, the crossing waters do not originate in the southern Ekman layer but rather in the southern *Sverdrup interior.*

Background. The idea of Ekman to deep water conversion in the northern ocean did not go unchallenged and, using numerical integrations, England and Rahmstorf (1999) argue that most of the Ekman-deep water conversion takes place in the South Atlantic and not the North Atlantic. This has some similarity to the idea presented earlier by Döös and Webb (1994) that the Ekman to deep water conversion takes place in stages rather than in one single step (such as the NADW formation). Related attempts to examine the role of the continuous zonal pressure gradient in the open Southern Ocean (or its absence) that should be mentioned here are those of McDermott (1996), Tsujino and Suginohara (1999) and Klinger et al. (2002). We shall argue that the question of what happens to the Ekman flux in the northern part of the Southern Ocean is not the right question to ask because these waters do not participate in the overturning drama.

The no Southern Ocean-Ekman flux across the equator idea presented in this article was already mentioned in passing in Nof (2000a) and in Nof (2002b). Here, we present it in a more explicit manner, and explain it in a way more suitable for a broader audience than that which typically reads the purely oceanographic literature.

Approach. We shall consider a simple single ocean basin similar to that considered in Nof (2000, 2002a,b) and focus on the case where all the convection occurs in the northern hemisphere (**Fig. 1**). We shall first present a general derivation of the wind-buoyancy transport formula assuming that the upper layer is continuously stratified and that there is a level-of-no-motion somewhere between 500 and 1500 m. We shall see later that the same transport formula can be derived even without making the level-of-no-motion approximation. Furthermore, we shall see that, with the Boussinesq approximation, the net meridional transport is determined by the wind regardless of the buoyancy flux. This means that the ocean's temperature and salinity fields will always adjust in such a way that the imposed buoyancy can be accommodated for (regardless of the meridional transport). This is followed by an analytical solution for the width of the trans-hemispheric stream and with numerical simulations. Finally, the results are discussed and summarized.

The belt model

Consider again the model shown in **Fig. 1** which contains four layers. An upper, continuously stratified, northward flowing layer contains the Ekman flow, the geostrophic flow underneath and the western boundary current. It is anywhere from 500 m to 1000 m thick where a level of no motion is assumed. The level-of-no-motion assumption coincides with a density surface but its depth varies in the field. Below this level the density is assumed to be constant. The upper moving layer contains both thermocline and some intermediate water, because some intermediate water is situated above the level-of-no-motion. It is subject to both zonal wind action and heat exchange with the atmosphere. The level-of-no-motion assumption is made merely for convenience and our results can also be obtained without it. In that case the vertical integration is done from the free surface to a fixed level just above the bottom topography.

Underneath the active layer there is a very thick (3000–4000 m) intermediate layer whose speeds [but not necessarily the transports (see e.g., Gill and Schumann, 1979)] are small and negligible. Underneath this thick layer there are two active layers which are not explicitly included

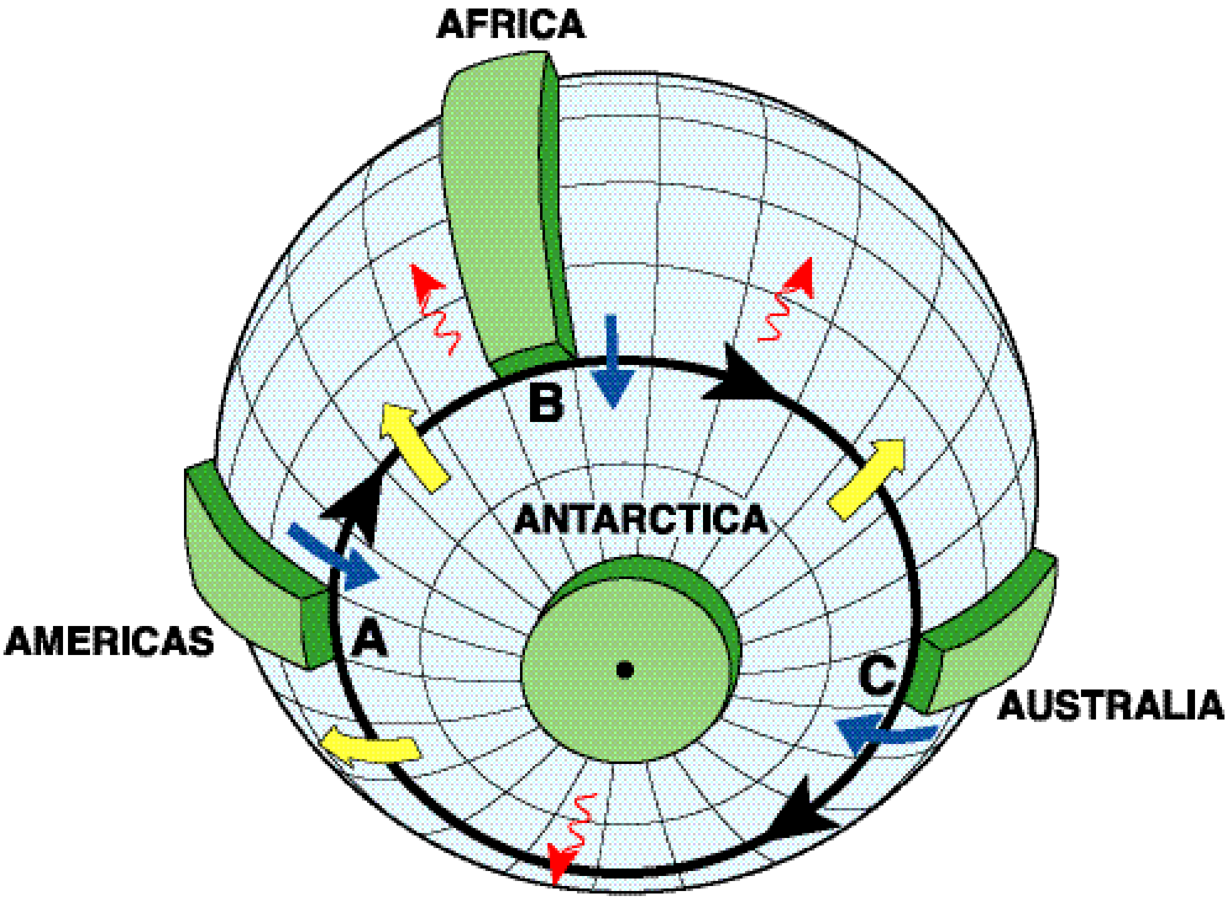

Fig. 1. Schematic diagram of the simplified geography used in Nof (2002b). The integration is done along a latitudinal circle passing through the southern tips of the continents (represented by the three peninsulas). The contour is situated inside a latitudinal corridor just *outside* the Antarctic Circumpolar Current (ACC) where the familiar linearized equations of motion are valid. Red "wiggly" arrows denote the net meridional mass flux. This net flow is a result of the manner by which the western boundary currents (narrow blue arrows) and the Sverdrup interior (thick yellow arrows) combine. For simplicity, we shall shortly combine the three peninsulas into one and speak about one ocean representing all three oceans (**Fig. 2**).

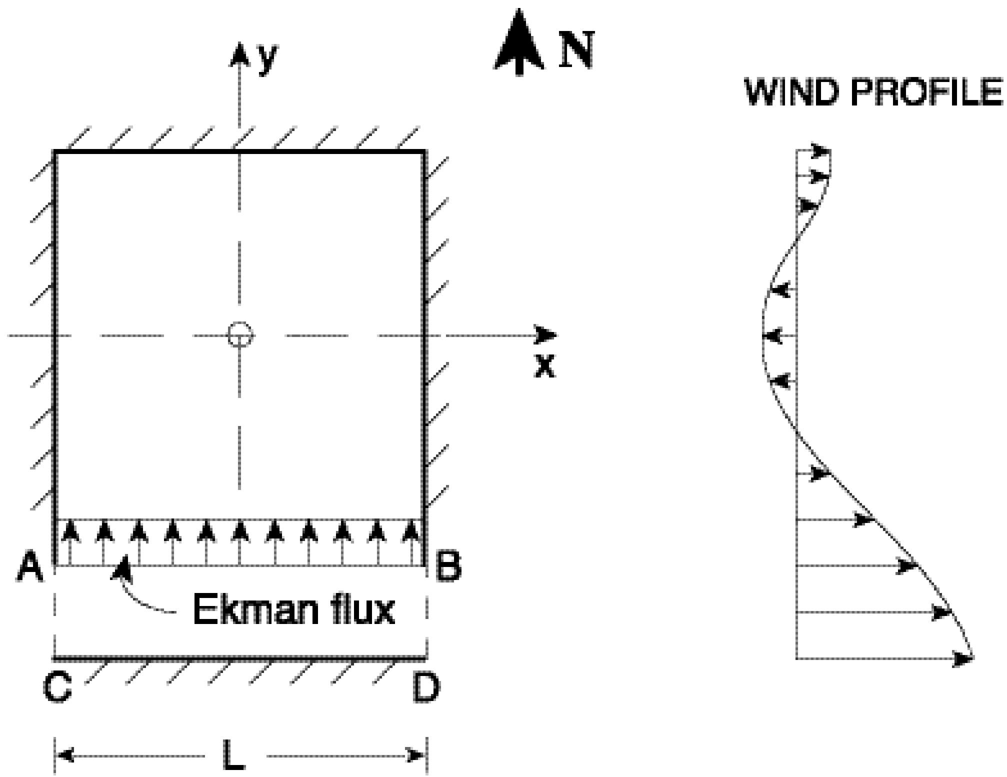

Fig. 2. Top view of the model where the three oceans shown in **Fig. 1** are combined into one. The single basin ocean has one moving layer overlaying a deep stagnant layer. The attached southern ocean has periodic boundary conditions at AC and BD. These periodic conditions represent the fact that the Southern Ocean encompasses the entire globe, requiring the pressure to be continuous. We shall see that across AB the wind pushes northward a flux of $\tau L/f_0$, where τ is the southern wind stress at AB. Buoyancy forces and deepwater formation must accommodate this northward flux. Note that the southern winds are considerably stronger than those in the northern hemisphere (right panel).

in the model and require a meridional wall to lean against. The first is the southward flowing layer which carries water such as the NADW; it is ~O(1000 m) thick. The second is the AABW layer whose thickness is ~O(100 m).

Vertical integration of the familiar linearized Boussinesq equations for the upper layer (subject to zonal winds) from the level-of-no-motion to the free surface gives,

$$-fV = -\frac{1}{\rho_0}\frac{\partial P^*}{\partial x} + \frac{\tau^x}{\rho_0} \tag{1}$$

$$fU = -\frac{1}{\rho_0}\frac{\partial P^*}{\partial y} - RV \tag{2}$$

$$\frac{\partial U}{\partial x} + \frac{\partial V}{\partial y} = 0 \quad , \tag{3}$$

where U and V are the vertically integrated transports in the x (eastward) and y (northward) directions, f is the Coriolis parameter (varying linearly with y), ρ_0 the uniform density of the motionless deep water, ρ the moving layer density [$\rho = \rho(x, y, z)$], P^* is the deviation of the integrated hydrostatic pressure from the integrated pressure associated with a state of rest, τ^x is the stress in the x direction, and R is an interfacial friction coefficient which, as we shall see, need not be specified for the purpose of our analysis. Friction is only included in the y momentum equation on the ground that it will be important only within the western boundary current (WBC), i.e., the analogous term RU does not appear in (1) because our region of interest is out of the Antarctic Circumpolar Current (ACC) so that U is small. The equations are valid for all latitudes including the equator. Elimination of the pressure terms between (1) and (2) and consideration of (3) gives,

$$\beta V = -\frac{1}{\rho_0}\frac{\partial \tau^x}{\partial y} - R\frac{\partial V}{\partial x} \quad , \tag{4}$$

which, for the inviscid ocean interior, reduces to the familiar Sverdrup relationship,

$$\beta V = -\frac{1}{\rho_0}\frac{\partial \tau^x}{\partial y} \quad , \tag{5}$$

Four comments should be made with regard to (1–5):

i. Thermohaline effects enter the equations through the deviation of the hydrostatic pressure from the pressure associated with a state of rest which is represented in P^*. They are not neglected in the model.

ii. Energy is supplied by both the wind and cooling; dissipation occurs through interfacial friction [i.e., the RV term in (2)] within the limits of the WBC system. Interfacial friction is not present in (1) because we assume that RU is small and negligible. Furthermore, since the velocities are small in the ocean interior the frictional term is taken to be negligible there.

iii. Relation (1) holds both in the sluggish interior away from the boundaries and in the intense WBC where the flow is geostrophic in the cross-stream direction. Within the WBC the balance is between the Coriolis and pressure terms with the wind stress playing a secondary role. In the interior, on the other hand, the velocities are small and, consequently, all three terms are of the same order.

iv. Since *there is a net meridional flow* in our model, the WBC transport is not equal and opposite to that of the Sverdup interior to its east. Furthermore, since the Sverdrup transport is fixed for a given wind field, it is the WBC that adjusts its transport to accommodate the net meridional transport imposed on the basin.

Integration of the momentum equation. We shall now simplify our analysis and combine our three oceans into one (**Fig. 2**). To derive the transport formula for the model, we follow Nof (2002b) and integrate (1) along the enclosed latitudinal circle shown in **Fig. 2**. Since the integral of the pressure term is identically zero, we immediately get,

$$-f_0 T = \int_A^C \left(\frac{\tau^x}{\rho_0}\right) dx \quad , \tag{6}$$

where T is the net meridional transport across the ocean and f_0 is the Coriolis parameter along the contour. The main point of this article is to show that, even though (6) looks like the familiar Ekman transport, it includes the Ekman flow, the geostrophic flow underneath and the transport of the WBC because both the equation and the region that we integrated across include those features. We shall see that much of the northward Ekman transport across our contour (**Fig. 2**) is flushed out of the basin via the recirculating gyres.

Relation (6) gives the combined (wind and cooling) transport in terms of the wind field and the geography alone. This means that cooling controls the local dynamics (i.e., where and how the sinking occurs as well as the total amount of downwelling and upwelling) but does not directly control the net amount of water that enters the ocean from the south. We shall return to this important point momentarily. Equation (6) can only be applied to a latitudinal belt "kissing" the tips of the continents. Away from the tips the ACC is established, and, consequently, form drag, friction, and eddy fluxes are no longer negligible and an RV term must be added to (1).

Since the interior is in Sverdrup balance, one immediately finds that, across AB, the width of the trans-hemispheric current, w, is,

$$w = \beta\tau L/f_0(\partial\tau/\partial y)\ , \qquad (7)$$

where L is the width of the basin. This condition is valid as long as the total Sverdrup transport across AB is greater than the transport pushed into the basin, i.e., $\partial\tau/\partial y > \beta\tau/f_0$. This is shown in **Fig. 3.** When $\partial\tau/\partial y$ is small (say, zero) then the entire trans-hemispheric transport occurs within the western boundary current (**Fig. 4**). This point will be addressed in detail shortly.

Numerical simulations

The methodology behind the numerical experiments is the same as that in Nof (2000, 2002a,b), i.e., we use a nonlinear reduced gravity model with the geometry shown in **Fig. 2**. The main point to note is that such a model will not reach a steady state without sources and sinks as it

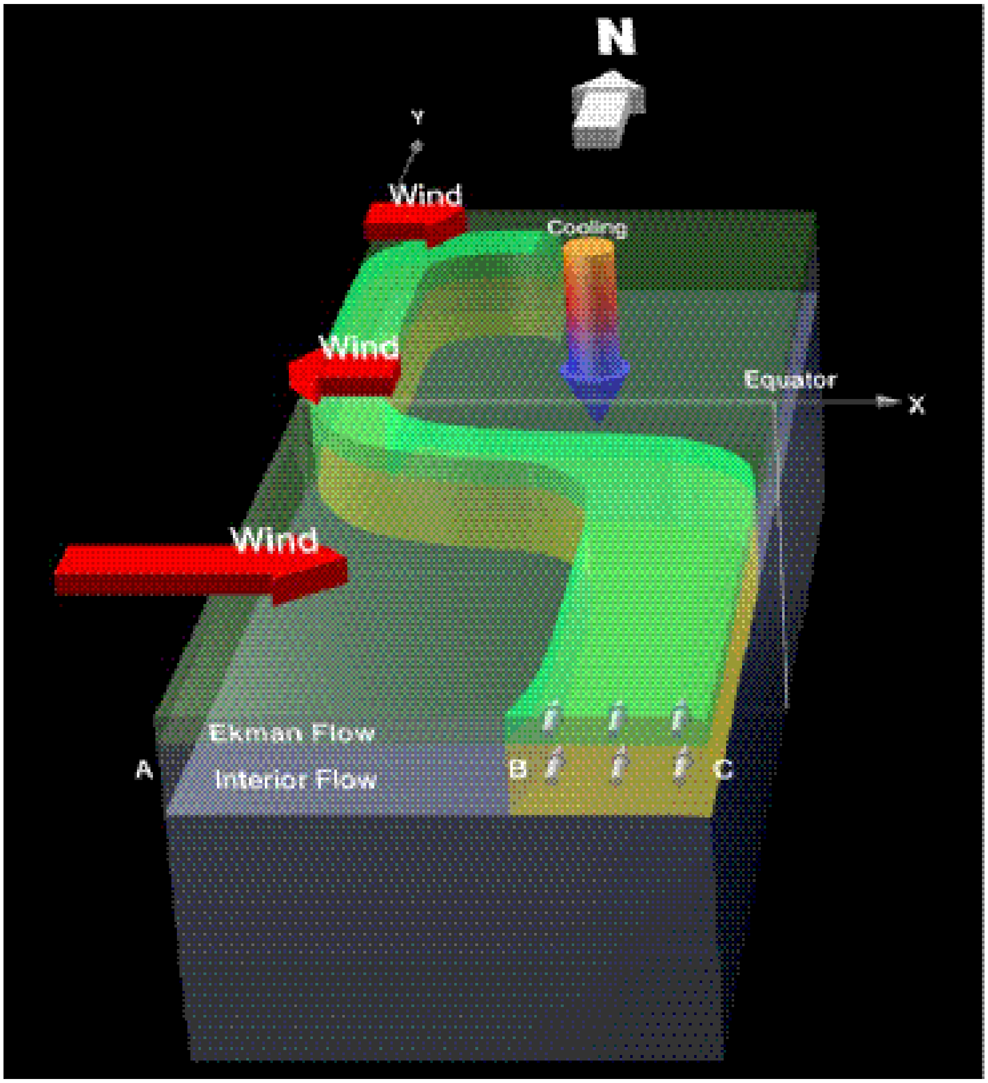

Fig. 3. The 3D path of Southern Ocean water to the north basin in the case where the wind stress curl is either moderate or strong (i.e., $\partial\tau/\partial y \neq 0$). Cross-section AC represents the southern edge of the basin. Most of the water that constitutes the "S" shaped path corresponds to interior geostrophic flow along the eastern southern boundary (and not to the southern Ekman flux). Here, both $\tau \neq 0$ and $\partial\tau/\partial y \neq 0$ along AC.

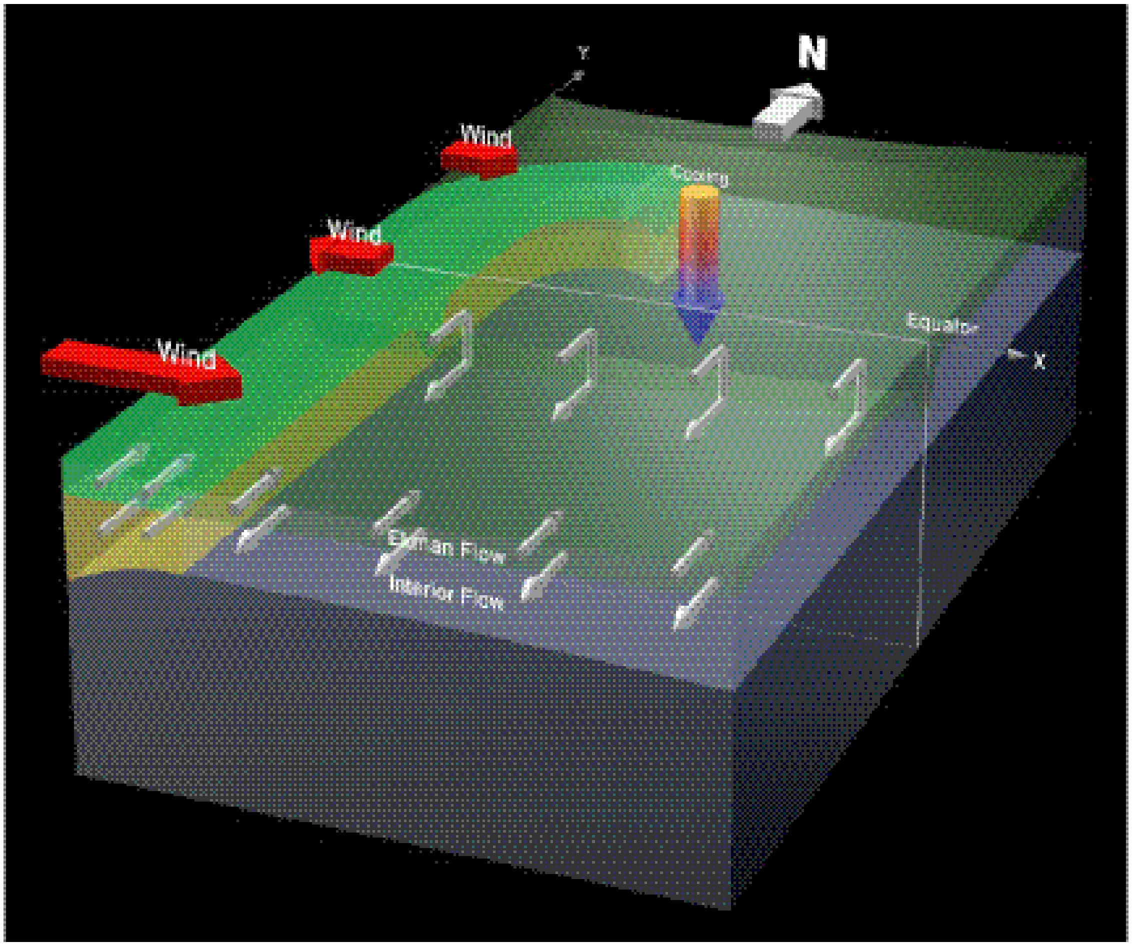

Fig. 4. The 3D path of southern hemisphere water to the northern hemisphere in the hypothetical case where there is no wind stress curl in the southern hemisphere, i.e., $\partial\tau/\partial y = 0$ everywhere but $\tau \neq 0$. Here, there is no net Sverdrup flow, i.e., the surface (southern) Ekman flux goes northward all the way to the equator where it sinks and returns southward as an interior geostrophic flow.

must obey (6) implying that meridional transport must be allowed. The purpose of the numerical simulations is to verify that there are no zonal jets emanating from the tip of the continents and that the zonal flow around Antarctica has no influence on the flow through the section. Such flows (see, e.g., Nof 2000b) could violate our momentum equations.

Instead of verifying the above general transport formula (6) using very complicated numerical models, we examined numerically the model (**Fig. 2**) that does not contain very complicated geography. Specifically, we considered a layer-and-a-half application of a "reduced gravity" isopycnic model. This numerical model has no thermodynamics, nor does it have enough layers to correctly represent the ACC. Neither of the two is essential and in order to represent the overturning we introduced two sources in the south and two sinks in the north. The mass flux associated with these sources and sinks is not *a priori* specified but the sources and sinks are required to handle an identical amount of water.

As in Nof (2000, 2002a,b), we let the wind blow, measured the transport established across section AB and then required the sources and sinks to accommodate this measured transport. We continued to do so and continued to adjust the transport until a steady state was ultimately reached. Note that, since our formula gives the transport without giving the complete flow field, it is easiest to start the above runs from a state of rest. Consequently, the initial adjustments that we speak about are not small but they do get smaller and smaller as we approach the predicted transport.

The numerical model. We used a reduced gravity version of the isopycnic model developed by Bleck and Boudra (1981, 1986), and later improved by Bleck and Smith (1990). The advantage of this model is the use of the "Flux Corrected Transport" algorithm (Boris and Book, 1973; Zalesak, 1979) for the solution of the continuity equation. This algorithm employs a higher order correction to the depth calculations and allows the layers to outcrop and stay positive definite. The resulting scheme is virtually non-diffusive and conserves mass. For these reasons, the model is the most suitable model for our problem.

The model uses the Arakawa (1966) C-grid. The u-velocity points are shifted one-half grid step to the left from the h points, the v-velocity points are shifted one-half grid step down from the h points, and the vorticity points are shifted one-half grid step down from the u-velocity points. This grid allows for reducing the order of the errors in the numerical scheme. The solution is advanced in time using the leap-frog scheme. The velocity fields are smoothed in time in order to stabilize the numerical procedure.

To make our runs more economical, we artificially magnified both β and the wind stress and artificially reduced both the meridional and zonal basin scales. The linear drag coefficient, K, was also increased so that the increased wind stress is balanced. With these modifications we had a dramatic reduction in the grid count and, consequently, our runs lasted for about 40 minutes each instead of a week or so that each run would have lasted had we not modified β, the wind stress and the basin's size. Note also that, even with our large frictional coefficient, the ratio between the Munk layer thickness $(\nu/\beta)^{1/3}$ and the basin size was still very small (as required) because our β is magnified.

Results. **Fig. 5** shows a typical experiment. In the shown case the numerical transport (nondimensionalized with $g'H^2/2f_{max}$) was 0.87 whereas the analytics gives a somewhat smaller amount of 0.77. Similarly, the theoretical width according to (7) is 0.59 whereas the simulated value is 0.60. All of our single ocean experiments are essentially a subset of the two basin experiments of Nof (2002b) because in his experiments the integrated zonal pressure gradient vanished for each individual basin. Hence, most of them are not reproduced here, and the very good numerical-theoretical agreement found there can also be regarded as the agreement here.

Fig. 5 also shows how the MOC crosses the equator. The water enters the southeastern Atlantic through the (linear) interior. It then follows an "S" shaped path and reaches the North Atlantic. One of the most important aspects of **Fig. 5** is that it shows very vividly that the waters entering the northern oceans are not Ekman fluxes but Sverdrup interior waters (along the eastern boundaries).

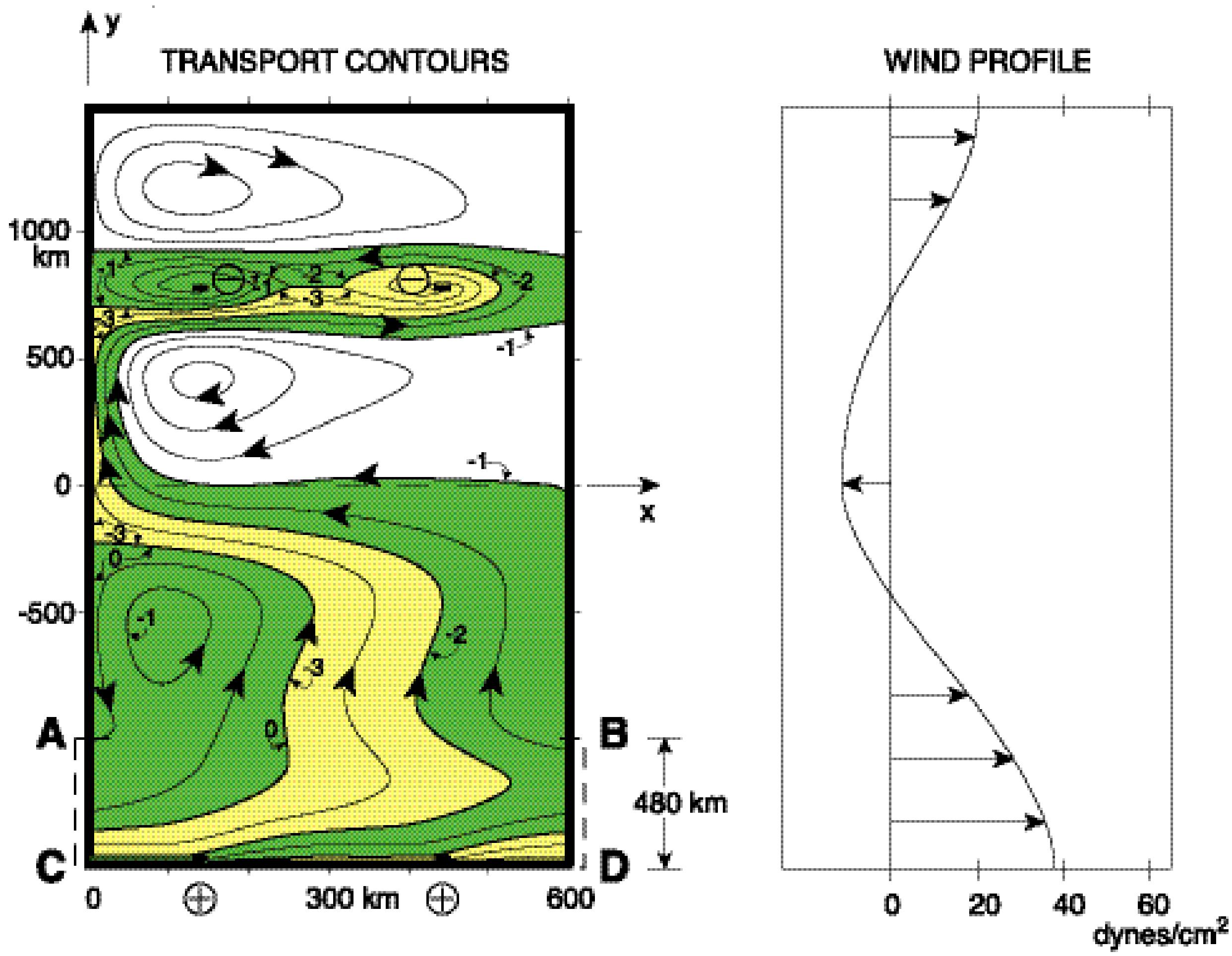

Fig. 5. The nondimensional transport contours for a typical numerical simulation with a rectangular basin subject to periodic boundary conditions at AC and BD.The sinks-sources mass flux is not determined *a priori*. Rather, the model itself determines the mass flux (see text). Also, note that the model does not include all the dynamics required for the ACC. Nevertheless, the model does have a tendency to produce such a current. The meridional flow forms an "S" shaped path. For this particular experiment the (nondimensionalized with the basin width) trans-hemispheric current width according to (6) is 0.59 whereas the displayed numerical value is slightly larger, 0.60. This relatively large ratio (of current width to basin width) is due to the large MOC transport relative to the Sverdrup transport. Parameters: $\Delta x = \Delta y = 15$ km; AT = 350 s; $R_d = 20$ km; $g' = 0.015$ ms^{-2}; H = 600 m; $\beta = 11.5 \times 10^{-11}$ m^{-1}s^{-1}; $\nu = 16{,}000$ m^{2}s^{-1}; K = 20×10^{-7}s^{-1}; $f_{max} = 1.5 \times 10^{-4}$s^{-1}; wind stress along the southern (northern) boundary is ~ 38 dynes/cm^2 (2.25 dynes/cm^2).

The meridional transport

Nof (2002b) used NCEP Reanalysis data[1] for annual mean winds (averaged over 40 years) with a drag coefficient of 1.6×10^{-3} [which is the appropriate coefficient for winds (such as ours) with a speed of less than 6.7 m s^{-1} (see e.g., Hellerman and Rosenstein (1983)]. Along the chosen path (**Fig. 1**), the integration was done over $2^\circ \times 2^\circ$ boxes. With the aid of (6) he found a reasonable net meridional transport of about 29 Sv (over the entire globe). According to the NCEP data for our contour, the winds do not vary much with longitude suggesting that the relative spacing between the continents can be used to divide the 29 Sv between the Atlantic (9 Sv) and the Pacific (20 Sv). It is not at all clear that the 20 Sv initially pushed into the Pacific does not ultimately recirculate into the South Atlantic (via the Agulhas and the ACC) but we shall assume here that only 9 Sv enter the Atlantic from the Southern Ocean.

Relation of (6) to the actual Ekman transport

At first glance, (6) and (7) may give the erroneous impression that the northward Ekman transport across the contour actually represents the MOC, i.e., that the fluid that starts in the Southern ocean and ends up in the northern hemisphere coincides with the Ekman transport across the contour shown in **Fig. 1**. A careful examination shows that this is not the case as the fluid that constitutes the MOC corresponds to either a fraction of the northward Sverdrup transport or a fraction of the WBC (rather than the Ekman transport). It is merely that the amount of water that is flowing northward is identical to the amount of the Ekman transport. To see this we first note that nowhere in our solution and its derivation has it ever been mathematically stated whether the flow belongs to the WBC, the Sverdrup interior or the Ekman flow. The only statement that has been made is that it is a combination of the three because (6) corresponds to an integrated quantity. We shall see that how the flow is partitioned between the Sverdrup and the WBC is determined by the

[1] Provided by the NOAA-CIRES Climate Diagnostics Center, Boulder, Colorado, from their Web site at http://www.cdc.noaa.gov.

wind stress curl which is not even present in (6). A strong or moderate curl implies an eastern current whereas a weak curl implies a western current.

We shall use two examples to show this. First, we shall look at the general case where the curl is strong so that there is a Sverdrup transport in the interior (**Fig. 6**) and then we shall look at the special case where the curl is weak, i.e., $\partial\tau/\partial y \equiv 0$ everywhere in the basin (**Figs. 7 and 4**). The second case is highly simplified and is, therefore, easier to understand. Some readers may prefer to look at it first.

Example 1: Consider the southern boundary of the basin and suppose, for a moment, that there is *no* MOC [i.e., the integral of (6) gives zero] so that the WBC transport (say, 40 Sv) is equal to and opposite that of the Sverdrup transport to the east (40 Sv). In this case $\tau = 0$ along our integration contour but $\partial\tau/\partial y$ is not zero. This is shown in the upper panel of **Fig. 6**. Next, consider the case where $\partial\tau/\partial y$ remains the same as before but τ is no longer zero along AB (lower panel). Suppose further that (6) gives 10 Sv for AB. Since the Sverdrup transport is fixed by the wind, the only way for the ocean to accommodate this northward transport of 10 Sv (imposed by the nonzero wind stress) is to weaken the WBC (from 40 to 30 Sv). The weakened WBC (**Fig. 6**, lower panel) still forms a recirculating gyre of 30 Sv with the western part of the Sverdrup transport (unshaded region) and, consequently, its fluid never leaves the southern hemisphere. The remaining Sverdrup transport (10 Sv) which does not participate in this recirculating gyre corresponds to the MOC, i.e., the fluid that ultimately crosses the equator and ends up in the northern hemisphere (shaded region). This is the fluid that we are interested in. It is situated next to the eastern boundary and corresponds to 1/4 of the total Sverdrup transport. This MOC transport is of the same amount as that given by the Ekman transport across AB but it obviously corresponds to a different water mass. Most of the Ekman transport across AB (the part between A and C) is advected by the fluid below in a manner that does not allow it to cross the equator, i.e., whatever enters this (unshaded) region is flushed back to the Southern Ocean.

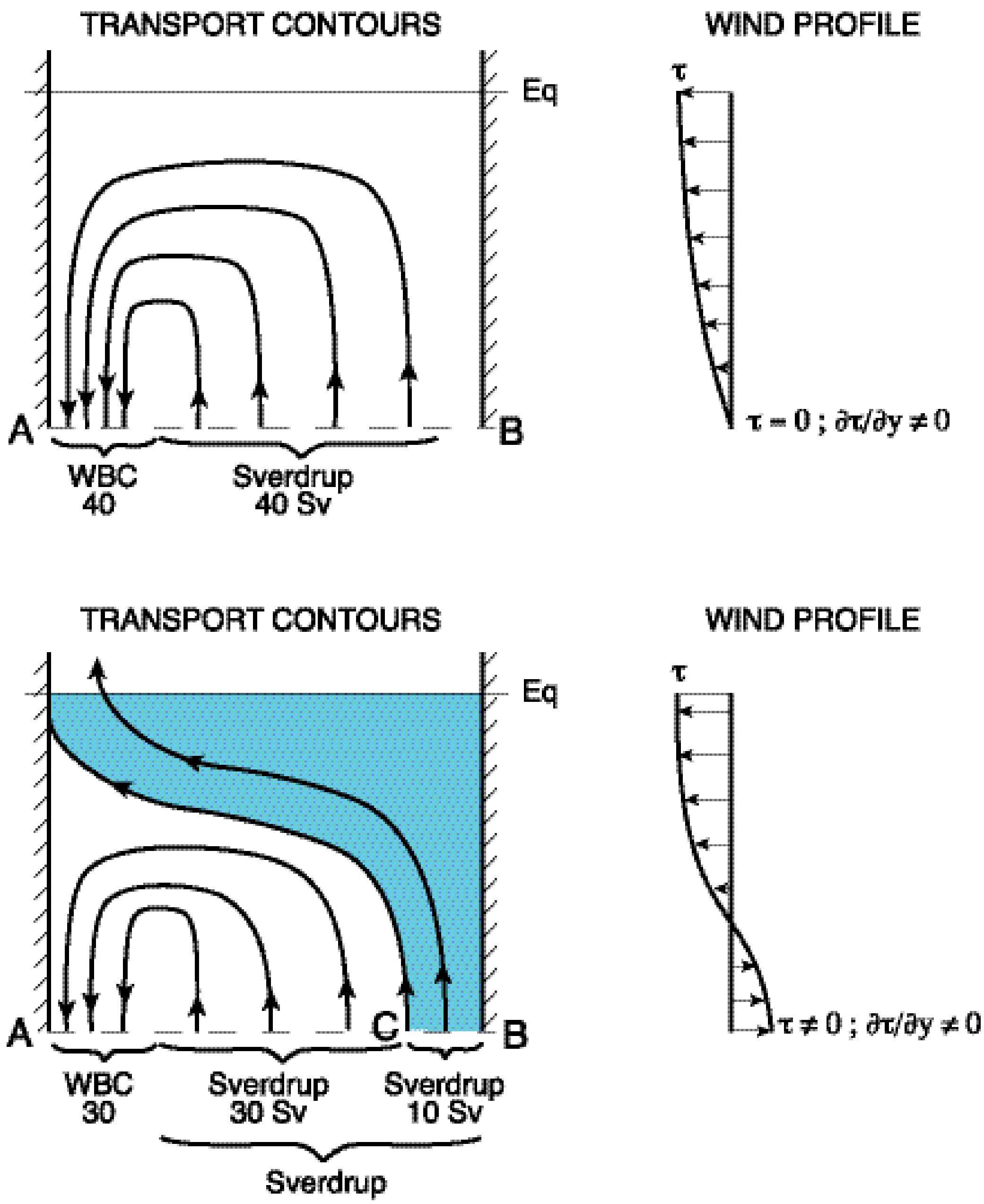

Fig. 6. A cartoon of the South Atlantic flow pattern in the vicinity of the integration contour. In the upper panel we show the case where (6) gives zero, i.e., there is no MOC and the WBC transport (say, 40 Sv) is equal and opposite to the Sverdrup flow. In the lower panel we show the case where the curl of the wind stress is the same as above but the integral of the wind stress across AB is now nonzero (and gives 10 Sv), i.e., there is an MOC. Since the Sverdrup balance is fixed by the wind, the only way for the ocean to accommodate the MOC is to weaken the WBC (from 40 to 30 Sv). As a result, the Sverdrup transport (still 40) is now greater than the WBC (30 Sv) and 10 Sv are now flowing northward along the eastern boundary. This 10 Sv ultimately ends up in the northern hemisphere. The northward flowing 10 Sv is also the calculated Ekman transport across AB but corresponds to a different water mass. Most of the Ekman flux across AB (i.e., the Ekman transport associated with AC) is advected by the fluid below in a circulatory manner and never crosses the equator because it is flushed out of the South Atlantic. Reproduced from Nof (2002b).

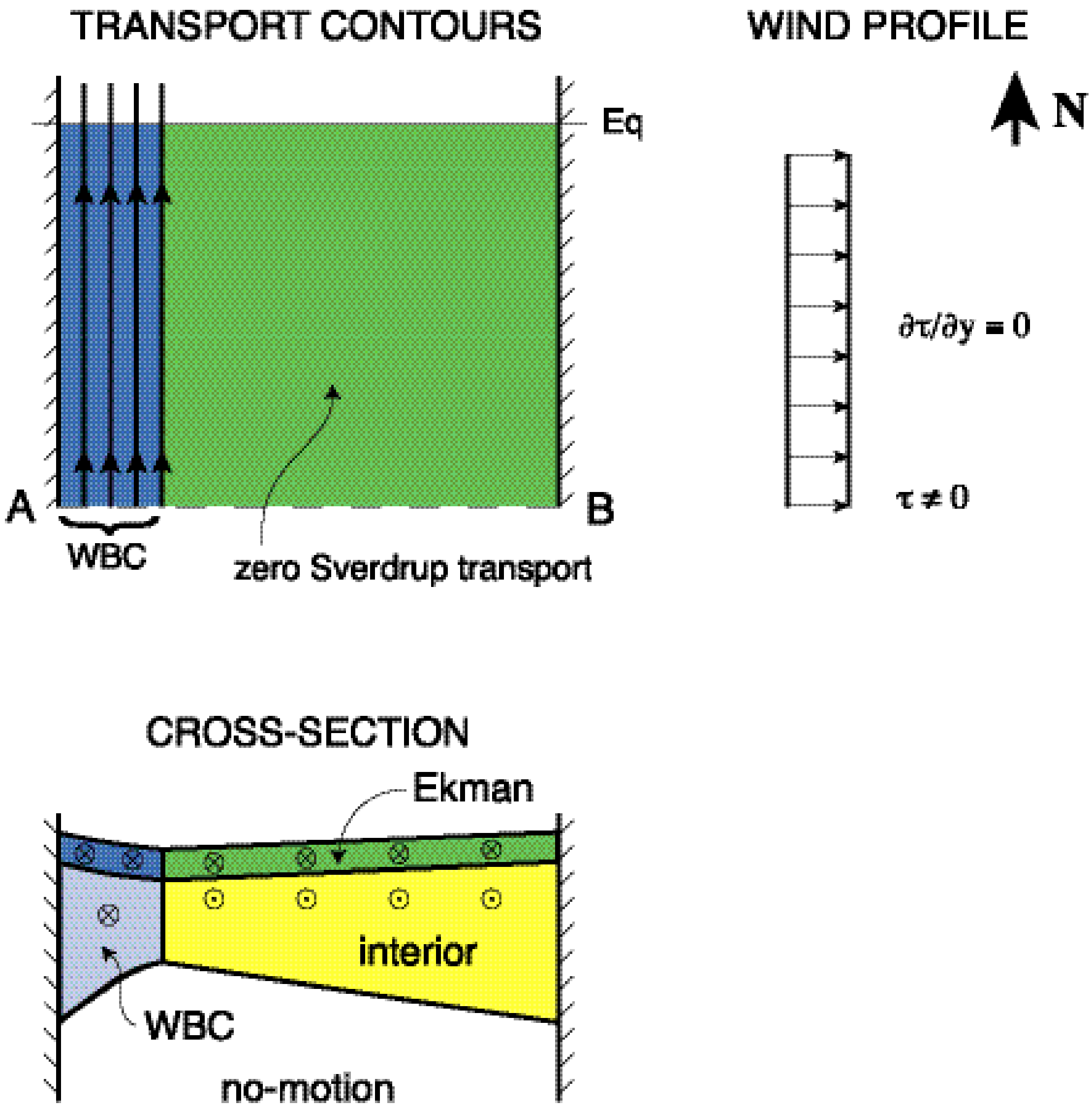

Fig. 7. The hypothetical (special) case of an MOC with no Sverdrup transport (i.e., $\tau \neq 0$ but $\partial\tau/\partial y = 0$ everywhere). Here again, most of the Ekman transport across AB (green) does not participate in the MOC drama even though the WBC transport (6) is the same as the Ekman transport. Since there is no net meridional transport east of the WBC, the northward Ekman transport there (10 Sv shown in green) cannot cross the equator, and hence, it sinks immediately to the south of it. This Ekman transport (green) is compensated for by a southward geostrophic flow immediately underneath (yellow). In turn, this interior flow underneath the Ekman layer (yellow) creates a compensating northward flowing WBC (light blue) which also carries 10 Sv. Namely, since the geostrophic interior flow must integrate to zero, the northward WBC is established to compensate for the southward geostrophic flow underneath the Ekman layer (yellow). Note that the amount of water associated with the Ekman flux within the WBC region (dark blue) is very small compared to the total Ekman flux (green plus dark blue) because the WBC is much narrower than the basin. Reproduced from Nof (2002b).

How is this reconciled with the fact that the integral of the geostrophic flow underneath the Ekman layer is zero? Very simply, the fact that there is no net flow in the geostrophic interior does not at all mean that the water that gets into the basin through AC is the *same* water that gets out via the WBC. All that it means is that there will be *some* water of the same amount that leaves through the interior. So, the amount of water going northward through AC (shaded region in the lower panel of **Fig. 6**) is *equal* to the Ekman transport across AC but constitutes a different water mass than the actual Ekman transport. As we have seen above, most of the entering Ekman transport is flushed back out of the South Atlantic (through the fluid below).

Example 2: Consider now the special (hypothetical) case of $\partial\tau/\partial y \equiv 0$ everywhere (no Sverdrup transport). Here, the MOC is flowing northward as a WBC with a transport equal to that of the Ekman transport across AB (**Figs. 7 and 4**). To see this, note that, since there is no Sverdrup transport east of the WBC, the northward Ekman transport there (10 Sv, shown in green) is compensated for by a southward transport of 10 Sv immediately underneath (yellow). Namely, the Ekman transport (green) proceeds meridionally all the way to the equator which acts like a wall (for the interior). Immediately south of the equator the Ekman layer thickness goes to infinity implying that the Ekman transport sinks and returns southward as an interior geostrophic flow (yellow).

Since the geostrophic interior transport must integrate across to zero, the southward transport underneath the Ekman layer (yellow) is compensated for by a northward WBC of 10 Sv (light blue). This WBC represents the MOC which ends up in the northern hemisphere. Again, although its transport is equal to that of the Ekman transport, it constitutes an entirely different water mass (i.e., blue rather than green). Note that the Ekman transport within the WBC (dark blue) is negligible compared to the total Ekman flux because the scale of the WBC is much smaller than the basin scale.

This completes the description of our two examples. A final point to be made is that the only time that (6) does coincide with the Ekman transport is when the width of the trans-hemispheric stream is identical to the basin width,

$$\int_A^B \frac{1}{\beta}\frac{\partial\tau}{\partial y}\,dx = \int_A^B \frac{\tau}{f_0}\,dx \quad ,$$

where A and B are shown in **Fig. 6**. In this hypothetical case the Ekman transport is identical to the Sverdrup transport because there is no flow at all in the geostrophic interior.

Concluding remarks

Using earlier theoretical considerations and earlier numerical simulations we illustrate that:

a. The upper layer mass flux of a wind-buoyancy driven meridional overturning cell originating in the Southern Ocean is given by $\tau L/f\rho$, where τ is the wind stress and L is the width of the basin.

b. This transport is, of course, equal to the Ekman transport into the basin but the actual trans-hemispheric current constitutes a different water mass. It corresponds to a Sverdrup flow along the eastern boundary (**Figs. 3, 5 and 6**). Its width is $\beta\tau L/f\ \partial\tau/\partial y$, where $\partial\tau/\partial y$ is the wind stress curl. For the South Atlantic the Sverdrup transport is 30 Sv whereas the MOC is roughly 10 Sv implying that 1/3 of the eastern South Atlantic corresponds to the trans-hemispheric exchange.

c. In the special case of no wind stress curl ($\partial\tau/\partial y \equiv 0$) but finite nonzero stress ($\tau \neq 0$), the entire trans-hemispheric flow takes place within the western boundary current (**Figs. 4 and 7**).

On this basis, it is suggested that the commonly used integrations of water properties across a latitudinal belt encompassing the entire globe and passing through the Southern Ocean should be interpreted with much caution. This is due to the fact that the Ekman flux which is a major component of these integrations does not participate in the interhemispheric mass-flux drama.

Acknowledgements

This study was supported by the National Science Foundation contract OCE 9911324; National Aeronautics and Space Administration grants NAG5-7630, NGT5-30164, and NAG5-10860; Office of Naval Research grant N00014-01-0291; and Binational Science Foundation grant 96-105. Discussions with G. Weatherly were very useful. Computations were done by S. Van Gorder; Figures 3 and 7 were prepared by Prem Subrahmanyam.

References

Arakawa, A., 1966. Computational design for long-term numerical integration of the equations of fluid motion. Two dimensional incompressible flow. Part I, *J. Comput. Phys.*, **1**, 119-143.

Bleck, R. and D. Boudra, 1981: Initial testing of a numerical ocean circulation model using a hybrid, quasi-isopycnic vertical coordinate. *J. Phys. Oceanogr.*, **11**, 744-770.

Bleck, R. and D. Boudra, 1986: Wind-driven spin-up in eddy-resolving ocean models formulated in isopycnic and isobaric coordinates. *J. Geophys. Res.*, **91**, 7611-7621.

Bleck, R. and L. T. Smith, 1990: A wind-driven isopycnic coordinate model of the North and Equatorial Atlantic Ocean, 1, Model development and supporting experiments. *J. Geophys. Res.*, **95**, 3273-3285.

Boris, J. P. and D. L. Book, 1973: Flux-corrected transport. I. SHASTA, a fluid transport algorithm that works. *J. Comput. Phys.*, **11**, 38-69.

Döös, K. and D. J. Webb, 1994: The Deacon cell and other meridional cells of the Southern Ocean. *J. Phys. Oceanogr.*, **24**, 429-442.

England, M. H. and S. Rahmstorf, 1999: Sensitivity of ventilation rates and radiocarbon uptake to subgrid-scale mixing in ocean models. *J. Phys. Oceanogr.*, **29**, 2802-2827.

Gill, A. E. and E. H. Schumann, 1979: Topographically induced changes in the structure of an inertial coastal jet: Application to the Agulhas Current. *J. Phys. Oceanogr.*, **9**, 975-991.

Hellerman, S. and M. Rosenstein, 1983: Normal monthly wind stress over the world ocean with error estimates. *J. Phys. Oceanogr.*, **13**, 1093-1104.

Klinger, B. A., J. P. McCreary, and R. Kleeman, 2002: The relationship between oscillating subtropical wind stress and equatorial temperature. *J. Phys. Oceanogr.*, **32**, 1507-1521.

McDermott, D., 1996: The regulation of Northern Hemisphere overturning by Southern Hemisphere winds. *J. Phys. Oceanogr.*, **26**, 1234-1255.

Nof, D., 2000: Does the wind control the import and export of the South Atlantic? *J. Phys. Oceanogr.*, **30**, 2650-2667.

Nof, D., 2002a: Is there a meridional overturning cell in the Pacific and Indian Oceans? *J. Phys. Oceanogr.*, **32**, 1947-1959.

Nof, D., 2000b: The Southern Ocean's grip on the northward meridional flow.. *Prog. in Oceanogr.*, in press.

Toggweiler, J. R. and B. Samuels, 1995: Effect of Drake Passage on the global thermohaline circulation. *Deep-Sea Res*., **42**, 477-500.

Tsujino, H. and N. Suginohara, 1999: Thermohaline circulation enhanced by wind forcing. *J. Phys. Oceanogr.*, **29**, 1506-1516.

Zalesak, S. T., 1979: Fully multidimensional flux-corrected transport algorithms for fluids. *J. Comput. Phys.*, **31**, 335-362.